

The Diagnostic Efficacy of MRI in the Evaluation of the Enlarged Vestibular Aqueduct in Children with Hearing Loss

Original Investigation

Fatma Ceren Sarioğlu¹ , Aslı Çakar Çetin² , Handan Gülyüz¹ , Enis Alpin Güneri²

¹Division of Pediatric Radiology, Department of Radiology, Dokuz Eylül University School of Medicine, İzmir, Turkey

²Department of Otorhinolaryngology, Dokuz Eylül University School of Medicine, İzmir, Turkey

Abstract

Objective: The aim of our study is to evaluate the diagnostic effectiveness of magnetic resonance imaging (MRI) compared to computed tomography (CT) in the detection of enlarged vestibular aqueduct (EVA) in childhood.

Methods: One hundred twenty-three children who underwent temporal bone CT and MRI examinations for hearing loss between 2013 and 2020 were evaluated retrospectively. All CT and MRI images were examined by two pediatric radiologists, according to the Valvassori and Cincinnati criteria for EVA. Imaging findings on CT and MRI of the vestibular aqueduct were recorded. Two pediatric radiologists performed the measurements for EVA on CT and MRI. In addition, an otolaryngologist performed the measurements independently. The sensitivity, specificity, positive predictive value (PPV), and negative predictive value (NPV) of MRI compared to CT were calculated to detect EVA. The difference between the measurements on CT and MRI was investigated. The inter-observer agreement was evaluated for measurements.

Results: The mean age of 123 children (65 boys and 58 girls) was 50.18±50.40 months. Two hundred for-

ty-six ears were evaluated in 123 children. On CT images, EVA was present in 28 (11.3%) of 246 ears according to Cincinnati criteria and 27 (10.9%) of 246 ears according to Valvassori criteria, respectively. While sensitivity, specificity, PPD, and NPD rates of MRI were 100%, 99%, 92.8%, and 100%, respectively, for Cincinnati criteria, for Valvassori criteria, they were 100%, 97.3%, 77.7%, and 100%, respectively. According to the visual evaluation performed without using measurement, the enlarged appearance of the vestibular aqueduct was significant for the diagnosis of EVA ($p<0.001$), while the absence of this appearance was significant for the exclusion of EVA ($p<0.001$). There was no significant difference between the measurements on CT and MRI. There was a perfect correlation between the observers for measurements.

Conclusion: MRI can be used as an initial imaging technique in children with suspicion of EVA to reduce radiation exposure.

Keywords: Magnetic resonance imaging, computed tomography, vestibular aqueduct, inner ear, diagnostic imaging, pediatric radiology

ORCID iDs of the authors:

F.C.S. 0000-0002-6714-2367;
A.Ç.Ç. 0000-0002-2549-0494;
H.G. 0000-0002-3205-4658;
E.A.G. 0000-0003-2592-0463.

Cite this article as: Sarioğlu FC, Çetin AÇ, Gülyüz H, Güneri EA. The Diagnostic Efficacy of MRI in the Evaluation of the Enlarged Vestibular Aqueduct in Children with Hearing Loss. *Türk Arch Otorhinolaryngol* 2020; 58(4): 220-6.

Introduction

Enlarged vestibular aqueduct (EVA) is one of the most frequent congenital inner ear abnormalities in children with sensorineural hearing loss (1). Valvassori and Clemis (2) have described the most commonly used criteria for determining the EVA in 1978. The term EVA refers to a greater diameter than 1.5 millimeters (mm) at the vestibular aqueduct's midpoint. Another definition of EVA, which has been introduced by Boston et al. (3) and called the Cincinnati criteria, is also widely used in daily clinical practice. According to Cincinnati

criteria, the EVA diagnosis is confirmed when the diameter of the vestibular aqueduct is greater than 2 mm in the operculum and/or 1 mm in the midpoint on the axial images.

Computed tomography (CT) provides a high spatial resolution allowing accurate measurements of the tiny temporal structures. Short acquisition time, which does not generally require sedation, is another advantage of CT. However, as is known, ionizing radiation is a major disadvantage associated with CT scans, especially in the pediatric age

Corresponding Author:
Fatma Ceren Sarioğlu, drcerenunal@gmail.com

Received Date: 08.08.2020

Accepted Date: 22.10.2020

Available Online Date: 28.10.2020

Content of this journal is licensed under a Creative Commons Attribution 4.0 International License. Available online at www.turkarchotolaryngol.net



DOI: 10.5152/tao.2020.5864

group. Children have a higher risk of leukemia and brain tumors due to ionizing radiation (4). Given the concern about exposure to ionizing radiation associated with CT scans, magnetic resonance imaging (MRI) has been proposed as an alternative first-line diagnostic tool for some common pathologies in children (5-7). Although CT has been accepted as the gold standard diagnostic tool in detecting inner ear abnormalities according to the previous literature (8), the advancing MRI technology has recently enabled a comprehensive evaluation of inner ear structures (9, 10). High resolution three-dimensional T2-weighted sequences allow visualization of small inner ear structures through exceptional image contrast between cerebrospinal fluid, vessels, and cranial nerves (10, 11).

This study aims to evaluate the diagnostic performance of MRI in detecting EVA in childhood. We aimed to reveal whether MRI would be an efficient first-line diagnostic test to detect EVA and ensure safety by avoiding ionizing radiation exposure in the pediatric age group.

Methods

Patients

The study was approved by the Institutional Review Board of Dokuz Eylül University School of Medicine (Protocol Number: GOA 2020/12-07). Written informed consent was obtained from the legal care-givers of all participants.

We retrospectively reviewed all pediatric patients (age range, 0-18 years) admitted to the Department of Otorhinolaryngology, Dokuz Eylül University School of Medicine, for hearing loss and underwent temporal bone CT and MRI between January 2013 and April 2020. Children diagnosed with unilateral or bilateral hearing loss, who were between 0-18 years old, and underwent temporal bone CT and temporal MRI were eligible. A child presenting with a temporal bone tumor invading the inner ear and 12 children whose radiological images included severe motion artifacts were excluded. Individuals with congenital cochleovestibular abnormalities, syndromic hearing loss, prenatally or postnatally acquired hearing loss were not further excluded because figuring out the EVA's presence or absence by using MRI was our primary purpose.

Main Points

- Magnetic resonance imaging offers high diagnostic performance for the diagnosis of enlarged vestibular aqueduct when using either the Cincinnati or Valvassori criteria.
- An enlarged-appearance of the vestibular aqueduct without using the measurements is a highly suggestive finding for the enlarged vestibular aqueduct. Also, the non-visible vestibular aqueduct's appearance is beneficial to exclude the diagnosis of the enlarged vestibular aqueduct on magnetic resonance imaging.
- We recommend using Magnetic resonance imaging as a first-step imaging technique in children with suspicion of an enlarged vestibular aqueduct to reduce the exposure of ionizing radiation.

Hearing assessment of the patients was carried out by a pure tone audiometer (GN Otometrics Madsen Astera², Taastrup, Denmark). The hearing loss was categorized as sensorineural hearing loss (SNHL), conductive hearing loss (CHL), and mixed hearing loss (MHL) for each ear separately, based on the recommendations of the Hearing Committee of the American Academy of Otolaryngology-Head and Neck Surgery (12). Finally, 123 children were enrolled in the study.

CT and MRI Protocol

Temporal bone CT images were obtained using a multi-detector CT scanner (Brilliance 64 Philips; Philips Medical Systems©, Eindhoven, The Netherlands). The field of view (FOV) was adjusted from the arcuate eminence to the mastoid tip. The acquisition parameters were as follows: slice thickness, 0.67 mm; slice interval, 0.33; pitch, 0.348; rotation time, 0.75 second (s); matrix, 768×768; FOV, 14×14 centimeters (cm); collimator, 20×0.625; 120 kilovolts (kV); 150 milliamperes (mA); bone algorithm reconstruction.

Temporal bone MRI images were obtained by a 1.5-Tesla MRI scanner (Gyrosan Achieva, release 8.1; Philips Medical Systems, Best, The Netherlands). In case of necessity, sedation was applied either orally or intravenously. Axial T1-weighted, axial and coronal T2-weighted, and axial T2-balance fast field echo (BFFE) weighted images were used for routine temporal MRI in our department for congenital sensorineural hearing loss. Contrast-enhanced images were also used in patients with acquired hearing loss. The features of imaging procedure were as follows: T1-weighted (time to repetition [TR], 500 milliseconds (ms); time to echo [TE], 15 ms; slice thickness, 3 mm; interslice gap, 0.5 mm; FOV, 20×20 cm; number of excitations [NEX], 3); T2-weighted (TR, 3300 ms; TE, 100 ms; slice thickness, 4 mm; interslice gap, 0.5 mm; FOV, 20×20 cm; NEX, 3); BFFE (TR, 6.8-7.3 ms; TE, 1.4-3.3 ms; slice thickness, 0.6 mm; FOV, 18×18 cm; NEX, 4).

Image Interpretation

Two pediatric radiologists, who have eight and 26 years of clinical experience in pediatric neuroradiology, read the CT and MRI images of 246 temporal bones. Then, the measurements were consulted by a ten-year experienced otorhinolaryngologist.

The radiologists, independent from each other, categorized the vestibular aqueducts' appearances on CT images based on their visual appearance (without any measurements) to correspond one of the enlarged, not enlarged, or suspiciously enlarged type (Figure 1). The midpoint and operculum measurements were performed for the enlarged and suspiciously enlarged types, as previously described (9, 13, 14), while no further measurements were required for the not enlarged types. The midpoint width was measured at the vestibular plane, which corresponds to the horizontal plane that the common dorsal crus arises from the vestibule. The opercular width referred to the maximum perpendicular vestibular aqueduct width at the operculum level. When the measurement met the Valvassori or Cincinnati criteria, the EVA diagnosis of that ear was confirmed.

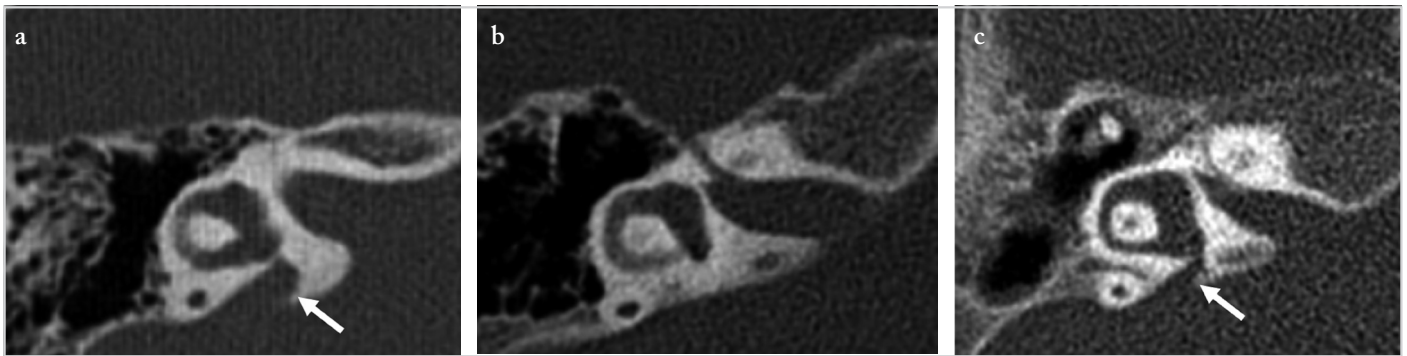


Figure 1. a-c. The classification of the vestibular aqueducts according to the visual analysis on CT scan. (a) The enlarged appearance of the vestibular aqueduct (arrow). (b) The non-enlarged vestibular aqueduct. (c) The vestibular aqueduct with suspicious enlargement (arrow)



Figure 2. a-c. The classification of the vestibular aqueducts according to the visual analysis on MRI. (a) The vestibular aqueduct with enlarged appearance (arrow). (b) The visible vestibular aqueduct without an enlarged appearance (thick arrow). The posterior semicircular canal (thin arrow). (c) The non-visible vestibular aqueduct. The posterior semicircular canal (arrow)

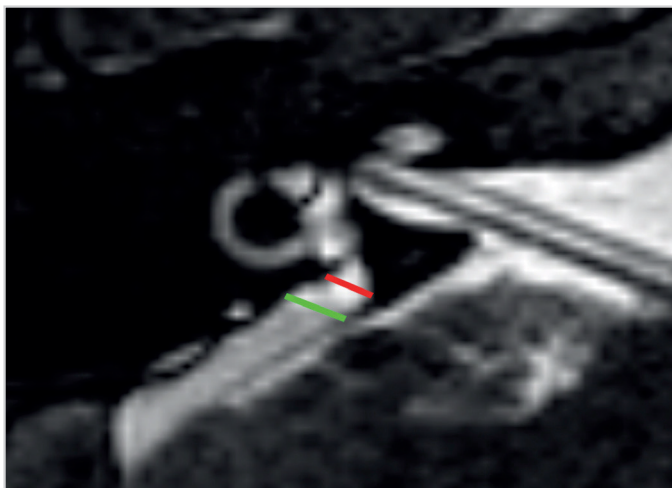


Figure 3. The measurements of the midpoint (red line) and operculum (green line) are demonstrated on the axial MRI image

The radiologists interpreted the MRI images three weeks after the CT evaluation. They classified the MRI findings of the vestibular aqueduct into three groups: the non-visible vestibular aqueduct, the visible vestibular aqueduct without an enlarged appearance, and the vestibular aqueduct with enlarged appearance (Figure 2). If the vestibular aqueduct was not visible, EVA was considered absent. For those ears with visible vestibular aqueducts (with enlargement or without enlargement), the width of vestibular aqueducts was identified by MRI (Figure 3).

The widths of the midpoint and operculum of the vestibular aqueducts were recorded. The ears were classified as EVA group and non-EVA group according to both the Cincinnati and the Valvassori criteria.

Statistical Analysis

Statistical analyses were performed with IBM Statistical Package for the Social Sciences version 22.0 (IBM SPSS Corp.; Armonk, NY, USA). Categorical variables and continuous numerical data were presented as frequency counts and percentages; and mean±standard deviation, respectively. The degree of inter-observer agreement was investigated by the intra-class correlation coefficient. Accordingly, poor, moderate, good, and excellent agreements were defined as the intra-class correlation coefficients to be less than 0.40, 0.41-0.60, 0.61-0.80, and greater than 0.80, respectively. Spearman's correlation coefficient was utilized to assess the correlation between the widths of the midpoint and operculum. The comparison between the EVA measurements obtained by CT and MRI was performed using the Independent Samples t-Test. The sensitivity, specificity, positive predictive value (PPV), and negative predictive value (NPV) of MRI in EVA diagnosis were calculated. Chi-square and Fisher's exact tests were used for evaluating the relationship between the EVA and imaging findings of MRI. A p-value of lesser than 0.05 was considered as statistically significant.

Results

A total of 123 children (65 boys and 58 girls) were enrolled in the study. The mean age was 50.18 ± 50.40 months (range, 3 to 192 months). Thirteen patients had unilateral hearing loss. Among 246 temporal bones in 123 patients, the frequencies of SNHL, CHL, and MHL were found to be 227 (92.2%), 1 (0.4%), and 5 (2%), respectively. Thirteen of 246 ears were presented with normal hearing (5.2%).

Eighteen of 246 vestibular aqueducts were enlarged, 23 of 246 showed a suspicious appearance for enlargement, and 205 of 246 were not enlarged according to the visual analysis on CT scans. When the Cincinnati criteria were followed as the gold standard on CT, 28 (ten of 23 ears showing a suspicious appearance for enlargement and all ears with enlarged-appearance) of 246 (11.3%) ears were included in the EVA group. On MRI, EVA was verified in 26 of those 28 ears (92.9%), which were diagnosed with EVA according to CT scans. The vestibular aqueducts of the remaining two ears with EVA were non-visible on MRI. None of the ears were false-positive for EVA on MRI. MRI had a sensitivity of 100%, a specificity of 99%, a PPV of 92.8%, and an NPV of 100% for detecting the EVA.

When the Valvassori criteria were followed, EVA was confirmed in 27 of 246 (10.9%) ears on CT images. One ear with a suspicious appearance for vestibular aqueduct enlargement on visual assessment was included in the EVA group according to the Cincinnati criteria, while assigned in the non-EVA group according to the Valvassori criteria (the widths of the midpoint and operculum were 1.2 and 3.3 mm, respectively) (Figure 4). Twenty-two of 27 ears (81.5%) with EVA were verified on MRI. The imaging findings of five ears with EVA, which could not be demonstrated on MRI, consisted of four ears with visible vestibular aqueducts without an enlarged appearance and one ear with a non-visible vestibular aqueduct. Another ear with a non-visible aqueduct on MRI, which was mentioned above, was not classified into the EVA group based on the Valvassori criteria. MRI had a sensitivity of 100%, a specificity of 97.3%, a PPV of 77.7%, and an NPV of 100% for detecting the EVA. The diagnostic performance of MRI was shown in Table 1.

The imaging findings of the vestibular aqueduct on MRI were summarized in Table 2. An enlarged appearance of the vestibular aqueduct on MRI (26 of 28 EVA ears (92.9%) according to the Cincinnati criteria and 22 of 27 EVA ears (81.5% according to the Valvassori criteria) was a significant indicator for

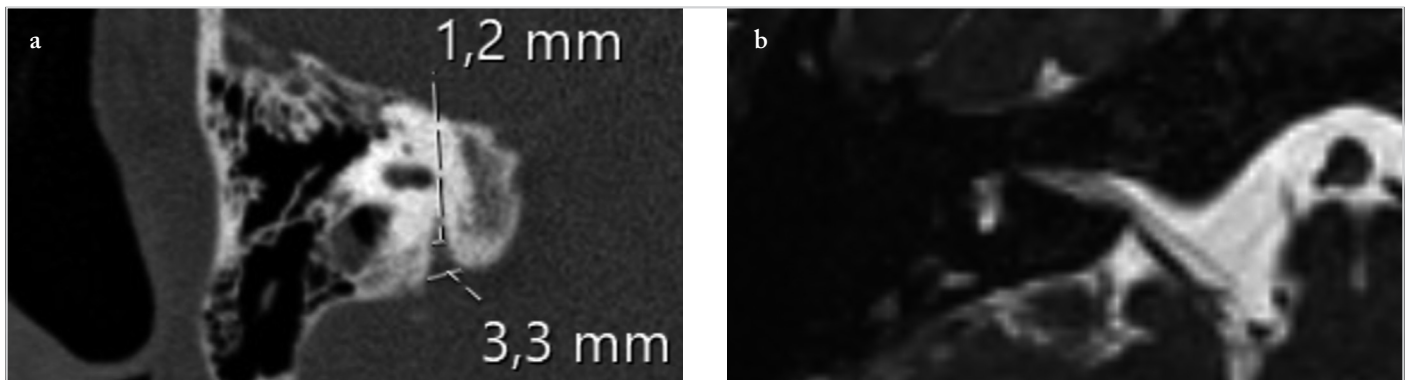


Figure 4. a, b. A patient with an ear included both in EVA and non-EVA groups according to the Cincinnati and Valvassori criteria, respectively. (a) On the CT scan, the midpoint and operculum widths were 1.2 and 3.3 mm, respectively. (b) The vestibular aqueduct was not visible on MRI. Please note that the semicircular canals are dysplastic

Table 1. The diagnostic performances of MRI in detecting EVA*

	Sensitivity (%)	Specificity (%)	PPV (%)	NPV (%)	Accuracy (%)
According to the Cincinnati criteria	100 (83.9-1)	99.0 (96.4-99.8)	92.8 (75.0-98.7)	100 (97.8-1)	99.1
According to the Valvassori criteria	100 (80.7-1)	97.3 (94.0-98.9)	77.7 (57.2-90.6)	100 (97.8-1)	97.5

*Numbers in parentheses are 95% confidence intervals (CI)

MRI: magnetic resonance imaging; EVA: enlarged vestibular aqueduct; PPV: positive predictive value; NPV: negative predictive value

Table 2. The appearances of the vestibular aqueducts on MRI

	According to the Cincinnati Criteria			According to the Valvassori Criteria		
	EVA group (n=28)	Non-EVA group (n=218)	p	EVA group (n=27)	Non-EVA group (n=219)	p
Non-visible	2 (7.1%)	193 (88.5%)	<0.001	1 (3.7%)	194 (88.6%)	<0.001
Visible but not enlarged	0 (0%)	25 (11.5%)		4 (14.8%)	25 (11.4%)	
Enlarged	26 (92.9%)	0 (0%)		22 (81.5%)	0 (0%)	

MRI: magnetic resonance imaging; EVA: enlarged vestibular aqueduct

Table 3. Inter-observer reliability

Measurements of the vestibular aqueduct	ICC	95% CI	p
At the midpoint on CT	0.991	0.980-0.996	<0.001
At the midpoint on MRI	0.975	0.946-0.988	<0.001
At the ostium on CT	0.981	0.960-0.991	<0.001
At the ostium on MRI	0.974	0.944-0.988	<0.001

ICC: intra-class correlation coefficient; CI: confidence interval. CT: computed tomography; MRI: magnetic resonance imaging

EVA ($p < 0.001$). The non-visible vestibular aqueduct (193 of 218 non-EVA ears (88.5%) according to the Cincinnati criteria and 194 of 219 non-EVA ears (88.6%) according to the Valvassori criteria) was a statistically significant indicator to exclude the diagnosis of EVA ($p < 0.001$) (Figure 1).

The inter-observer reliability results between the otorhinolaryngologist and radiologists for the measurements of the vestibular aqueduct on CT scan and MRI are summarized in Table 3. Excellent inter-observer agreements were obtained. The values provided by the radiologists represented the mean values. The mean midpoint width was 3.02 ± 1.06 and 2.57 ± 1.20 on CT and MRI, respectively. The mean operculum width was 5.15 ± 1.87 and 4.35 ± 2.06 on CT and MRI, respectively. There were no significant differences regarding the midpoint ($p = 0.061$) and operculum ($p = 0.053$) between CT and MRI. There were excellent correlations between the measurements of the midpoint and operculum on the CT and MRI ($p < 0.001$; $Rho = 0.826$, $p < 0.001$; $Rho = 0.899$, respectively).

Discussion

Currently, there has been no consensus on which initial imaging modality should be performed in children who are clinically suspicious for the presence of EVA. Despite the well-known and widely-used CT-based diagnostic criteria, we investigated the potential diagnostic capability of MRI in EVA due to our concerns about exposure to CT-based ionizing radiation in children. Our results indicated that MRI was quite valid to diagnose EVA with a sensitivity of 100% and a specificity of 97-99%. The NPV values of MRI were 100% for both of the criteria. The non-visible vestibular aqueduct was an indicator to exclude EVA on MRI. Moreover, a vestibular aqueduct with enlarged appearance on MRI was found to be a significant parameter for detecting EVA according to the Cincinnati (92.9%) and Valvassori criteria (81.5%).

Only a few studies have evaluated the diagnostic capability of MRI in comparison to CT to diagnose EVA (9, 15). In 1997, Dahlen et al. (15) reported that 33 of 38 ears (86.8%) were positive for EVA on MRI. However, they suggested that MRI is a complementary imaging tool to CT in the diagnosis of EVA due to its false-positive and false-negative results. A recent study conducted by Connor et al. (9) observed no differences between the vestibular aqueduct measurements using CT and MRI in children with EVA. They defined the diagnostic agreement for CT and MRI to be 93%. They demonstrated that a few false-positive and false-negative cases were

present on MRI. We did not find any false-positive findings on MRI. According to our results, the enlarged appearance of the vestibular aqueduct on MRI was correlated with EVA diagnosis, which was confirmed by either the Valvassori or the Cincinnati criteria. Hence, we suggest the use of MRI as a first-step diagnostic tool instead of a CT scan to exclude EVA and to perform a CT scan if required for those cases with high clinical suspicion of EVA in pediatric age. Although MRI has high diagnostic accuracy and NPV according to our results, considering the pediatric age group, we recommend not to underestimate the potential necessity of sedation or anesthetic administration to maintain the stability of positioning during the long acquisition time of MRI, and we highlight this as a limitation.

CT has a high spatial resolution, which means the capability of distinguishing two small, discrete objects (16). In the literature, vestibular aqueducts' measurements showed lower values on MRI than CT, though there were not any statistically significant differences (9, 15). It has been proposed that the lower values on MRI might be related to the challenges of distinguishing between the tip of the thin bony operculum and dura. Besides, a transient enlargement of the fluid space that resulted in a widening of the vestibular aqueduct has also been suggested as another theory to explain these differences (9, 15). Our results were compatible with the literature. Another strength of our study was the reliability of the measurements between two independent assessors. The inter-observer reliability was excellent when the measurements performed on CT and MRI by the otorhinolaryngologist versus pediatric radiologists.

The vestibular aqueduct's normative measurements have been studied in different planes of the temporal bone previously (2, 3, 17-19). Although the classical methods were described in the Valvassori and Cincinnati criteria, the adjacent posterior semicircular canal's width was also used as a standard reference. Also, Juliano et al. (17) revealed that the vestibular aqueduct's normative diameter in the 45° oblique reformat plane was 0.5 mm (0.3-0.9 mm) at the midpoint. Ozgen et al. (18) found that the 45° oblique plane on CT scan was more reliable for measuring the vestibular aqueduct than the axial plane. The 45° oblique plane was not used in this study since reformat images would be useful solely on CT scan, not MRI. Therefore, an optimal comparison between CT and MRI could not be achieved.

EVA can occur either as an isolated abnormality or accompany by other congenital conditions (20). Associated abnormalities should be meticulously clarified, especially in the preoperative assessment of cochlear implant candidates. Many authors investigated the benefit of using preoperative MRI and CT in pediatric cochlear implant candidates (21-24). They concluded that CT was superior to MRI to identify the temporal bone abnormalities, whereas MRI played a critical role when demonstrating cochlear nerve pathologies and accompanied intracranial morbidities. Nevertheless, they also found many overlaps between the two imaging modalities. Trimble et al. (21) suggested a selective use of both imaging modalities within a diagnostic algorithm. Parry et al. (22) suggested the use of MRI in the first-step evaluation in cochlear implant candidates and to continue with the use of CT if required, such as in the case of suspicion for bony abnormalities. Unlike these results, Gleeson et al. (23) demonstrated that the combined use of CT and MRI was not superior to either modality alone.

The exact incidence of EVA in children is still unknown. However, it has been reported to distribute in a wide range from %0.6 to 10% (19, 25-28). The differences regarding the studies may be due to different factors such as the age of the sample size, imaging techniques, and the evaluation methods. Besides, detecting this abnormality has been improved day by day following the advances in imaging technology. Besides, SNHL, which is known to be the most common clinical manifestation in patients with EVA, has become more detectable in the younger age groups due to universal newborn hearing screening programs. In our study, 11% of the 246 temporal bones had EVA. Our study's high incidence rate may be related to our patient cohort, most of which presented with SNHL (227 of 246 ears [92.2%]).

We agree that the relatively small sample size, the retrospective design, and the lack of vestibular assessment are among the limitations of our study. However, we also wish to remind that evaluating vestibular symptoms in the pediatric age group may be extremely challenging.

Conclusion

MRI has high diagnostic accuracy in EVA when using either the Cincinnati or the Valvassori criteria. The non-visible vestibular aqueduct on MRI is a useful marker to exclude EVA. We believe that our results will make valuable contributions to EVA's diagnostic algorithm in otolaryngologists and radiologists' daily clinical practice. Because it does not necessitate the use of ionizing radiation, MRI may offer a safe and effective diagnostic property in diagnosing EVA in children as a first-step diagnostic tool. Further research is also needed to determine the cost-effectiveness and feasibility of implementing MRI on a large scale.

Ethics Committee Approval: Ethics committee approval was received for this study from the Institutional Review Board of Dokuz Eylül University School of Medicine (Protocol Number: GOA 2020/12-07).

Informed Consent: Written informed consent was obtained from the legal care-givers of all patients who participated in this study.

Peer-review: Externally peer-reviewed.

Author Contributions: Concept - F.C.S., A.Ç.Ç., H.G., E.A.G.; Design - F.C.S., A.Ç.Ç., H.G., E.A.G.; Supervision - H.G., E.A.G.; Materials - F.C.S., A.Ç.Ç., H.G.; Data Collection and/or Processing - F.C.S., A.Ç.Ç., H.G., E.A.G.; Analysis and/or Interpretation - F.C.S., A.Ç.Ç., H.G., E.A.G.; Literature Search - F.C.S.; Writing - F.C.S.; Critical Reviews - A.Ç.Ç., H.G., E.A.G.

Conflict of Interest: The authors have no conflicts of interest to declare.

Financial Disclosure: The authors declared that this study has received no financial support.

References

1. Mafee MF, Charletta D, Kumar A, Belmont H. Large vestibular aqueduct and congenital sensorineural hearing loss. *AJNR Am J Neuroradiol* 1992; 13: 805-19.
2. Valvassori GE, Clemis JD. The large vestibular aqueduct syndrome. *Laryngoscope* 1978; 88: 723-8.
3. Boston M, Halsted M, Meinzen-Derr J, Bean J, Vijayasekaran S, Arjman E, et al. The large vestibular aqueduct: a new definition based on audiologic and computed tomography correlation. *Otolaryngol Head Neck Surg* 2007; 136: 972-7.
4. Pearce MS, Salotti JA, Little MP, McHugh K, Lee C, Kim KP, et al. Radiation exposure from CT scans in childhood and subsequent risk of leukaemia and brain tumours: a retrospective cohort study. *Lancet* 2012; 380: 499-505.
5. Kinner S, Pickhardt PJ, Riedesel EL, Gill KG, Robbins JB, Kitchin DR, et al. Diagnostic accuracy of MRI versus CT for the evaluation of acute appendicitis in children and young adults. *AJR Am J Roentgenol* 2017; 209: 911-9.
6. Eng KA, Abadeh A, Ligocki C, Lee YK, Moineddin R, Adams-Webber T, et al. Acute appendicitis: a meta-analysis of the diagnostic accuracy of US, CT, and MRI as second-line imaging tests after an initial US. *Radiology* 2018; 288: 717-27.
7. Lindberg DM, Stence NV, Grubenhoff JA, Lewis T, Mirsky DM, Miller AL, et al. Feasibility and accuracy of fast MRI versus CT for traumatic brain injury in young children. *Pediatrics* 2019; 144: e20190419.
8. Joshi VM, Navlekar SK, Kishore GR, Reddy KJ, Kumar EC. CT and MR imaging of the inner ear and brain in children with congenital sensorineural hearing loss. *Radiographics* 2012; 32: 683-98.
9. Connor SEJ, Dudau C, Pai I, Gaganasiou M. Is CT or MRI the optimal imaging investigation for the diagnosis of large vestibular aqueduct syndrome and large endolymphatic sac anomaly? *Eur Arch Otorhinolaryngol* 2019; 276: 693-702.
10. Oh JH, Chung JH, Min HJ, Cho SH, Park CW, Lee SH. Clinical application of 3D-FIESTA image in patients with unilateral inner ear symptom. *Korean J Audiol* 2013; 17:111-7.
11. Cavusoglu M, Ciliz DS, Duran S, Ozsoy A, Elverici E, Karaoglanoglu R, et al. Temporal bone MRI with 3D-FIESTA in the evaluation of facial and audiovestibular dysfunction. *Diagn Interv Imaging* 2016; 97: 863-9.
12. Gurgel RK, Jackler RK, Dobie RA, Popelka GR. A new standardized format for reporting hearing outcome in clinical trials. *Otolaryngol Head Neck Surg* 2012; 147: 803-7.

13. Vijayasekaran S, Halsted MJ, Boston M, Meinzen-Derr J, Bardo DME, Greinwald J, et al. When is the vestibular aqueduct enlarged? A statistical analysis of the normative distribution of vestibular aqueduct size. *AJNR Am J Neuroradiol* 2007; 28: 1133-8.
14. Dewan K, Wippold FJ 2nd, Lieu JE. Enlarged vestibular aqueduct in pediatric sensorineural hearing loss. *Otolaryngol Head Neck Surg* 2009; 140: 552-8.
15. Dahlen RT, Harnsberger HR, Gray SD, Shelton C, Allen R, Parkin JL, et al. Overlapping thin-section fast spin-echo MR of the large vestibular aqueduct syndrome. *AJNR Am J Neuroradiol* 1997; 18: 67-75.
16. Wang J, Fleischmann D. Improving spatial resolution at CT: development, benefits, and pitfalls. *Radiology* 2018; 289: 261-2.
17. Juliano AF, Ting EY, Mingkwansook V, Hamberg LM, Curtin HD. Vestibular aqueduct measurements in the 45° oblique (Pöschl) plane. *AJNR Am J Neuroradiol* 2016; 37: 1331-7.
18. Ozgen B, Cunnane ME, Caruso PA, Curtin HD. Comparison of 45 degrees oblique reformats with axial reformats in CT evaluation of the vestibular aqueduct. *AJNR Am J Neuroradiol* 2008; 29: 30-4.
19. Saliba I, Gingras-Charland ME, St-Cyr K, Décarie JC. Coronal CT scan measurements and hearing evolution in enlarged vestibular aqueduct syndrome. *Int J Pediatr Otorhinolaryngol* 2012; 76: 492-9.
20. Ho ML, Moonis G, Halpin CF, Curtin HD. Spectrum of third window abnormalities: semicircular canal dehiscence and beyond. *AJNR Am J Neuroradiol*. 2017; 38: 2-9.
21. Trimble K, Blaser S, James AL, Papsin BC. Computed tomography and/or magnetic resonance imaging before pediatric cochlear implantation? Developing an investigative strategy. *Otol Neurotol* 2007; 28: 317-24.
22. Parry DA, Booth T, Roland PS. Advantages of magnetic resonance imaging over computed tomography in preoperative evaluation of pediatric cochlear implant candidates. *Otol Neurotol*. 2005; 26: 976-82.
23. Gleeson TG, Lacy PD, Bresnihan M, Gaffney R, Brennan P, Viani L. High resolution computed tomography and magnetic resonance imaging in the pre-operative assessment of cochlear implant patients. *J Laryngol Otol* 2003; 117: 692-5.
24. Kanona H, Stephenson K, D'Arco F, Rajput K, Cochrane L, Jephson C. Computed tomography versus magnetic resonance imaging in paediatric cochlear implant assessment: a pilot study and our experience at Great Ormond Street Hospital. *J Laryngol Otol* 2018; 132: 529-33.
25. Emmett JR. The large vestibular aqueduct syndrome. *Am J Otol* 1985; 6: 387-415.
26. Fahy CP, Carney AS, Nikolopoulos TP, Ludman CN, Gibbin KP. Cochlear implantation in children with large vestibular aqueduct syndrome and a review of the syndrome. *Int J Pediatr Otorhinolaryngol* 2001; 59: 207-15.
27. Arjmand EM, Webber A. Audiometric findings in children with a large vestibular aqueduct. *Arch Otolaryngol Head Neck Surg* 2004; 130: 1169-74.
28. Koesling S, Rasinski C, Amaya B. Imaging and clinical findings in large endolymphatic duct and sac syndrome. *Eur J Radiol* 2006; 57: 54-62.